

Locally resolved ^1H Knight shifts and the order-disorder phase transition in the organic conductor N,N -dimethyl-thiomorpholinium bis-tetracyanoquinodimethane $[\text{DMTM}(\text{TCNQ})_2]$

A. C. Kolbert and G. Zimmer

2. Physikalisches Institut, Universität Stuttgart, Germany

F. Rachdi and P. Bernier

Groupe de Dynamique des Phases Condensées, U.S.T.L., 34095 Montpellier, France

M. Almeida

Departamento Quimica, ICEN, LNETI, 2686 Sacavem Codex, Portugal

M. Mehring

2. Physikalisches Institut, Universität Stuttgart, Germany

(Received 24 October 1991)

The electronic and dynamic changes through the phase transition in the organic conductor N,N -dimethyl-thiomorpholinium bis-tetracyanoquinodimethane $[\text{DMTM}(\text{TCNQ})_2]$ have been investigated with use of ^1H nuclear magnetic resonance. Proton Knight shifts have been measured with multiple-pulse, magic-angle spinning NMR as a function of temperature. Three inequivalent TCNQ ^1H lines were observed above the phase transition at 272 K, and eight below, all with negative Knight shifts, ranging from -20 to -75 ppm, in the temperature range 190–300 K, representing an extremely large observed ^1H Knight shift. The isotropic hyperfine coupling constants and corresponding spin densities were calculated, and an estimate of the charge redistribution at T_c , based upon a tentative assignment of the lines, is made. The cation dynamics were also investigated with broadline ^1H NMR which indicate a slowing of the DMTM-cation motion upon cooling through the phase transition, while relaxation measurements in the rotating frame indicate a cooperative phenomenon involving slow motions at T_c . All of these results are considered in terms of the structural changes at the phase transition.

I. INTRODUCTION

The organic conductor N,N -dimethyl-thiomorpholinium bis-tetracyanoquinodimethane $[\text{DMTM}(\text{TCNQ})_2]$ has attracted a great deal of attention lately because of its unusual structural phase transition.^{1–6} Upon cooling through $T_c = 272$ K, the conductivity increases by a factor of 500, a behavior which is inverted with respect to the behavior of the common charge-transfer salts.² The relationship between the structural changes at the phase transition and the conductivity anomaly is still unclear, however. The complete crystal structure has been determined, by x-ray diffraction, above the phase transition—the unit cell is monoclinic with space group $P2_1/m$, and the DMTM cation is located on a mirror plane between two equivalent sheets of parallel, dimerized TCNQ stacks.^{1,6} The complete structure below T_c has not yet been performed because of the tendency of the crystals to twin at the phase transition, though some features are known.⁶ The structure changes to triclinic (space group $P1$ or $P\bar{1}$), and the two TCNQ stacks are no longer crystallographically equivalent. The presence of a mirror plane, on which the DMTM's are located, and its subsequent loss suggest that the cations are either statically or dynamically disordered above the phase transition and, in some way, ordered below it.^{1,6} The directed dipole mo-

ment of the ordered cation could conceivably lead to interstack electron transfer, tentatively proposed as an explanation for the conductivity anomaly.¹

The measurement of Knight shifts⁷ in the nuclear-magnetic-resonance (NMR) spectra of organic conductors has been shown to yield important information concerning the electronic conduction, in some cases yielding a locally resolved spin-density map of the conduction-band orbital.^{8,9} Some high-resolution ^{13}C studies of Knight shifts in organic conductors have been performed,^{9–13} but ^1H NMR has been utilized much less frequently. This is unfortunate, as proton Knight shifts are more easily interpreted than ^{13}C Knight shifts, since contributions due to chemical shifts are smaller and the relationship between Knight shifts and spin densities is more direct. Furthermore, ^1H is 100% naturally abundant, and complete studies can be made without the need for isotopic enrichment, as is often required for ^{13}C . The reason for the paucity of ^1H results in the literature is that the ^1H spectra of organic systems are dominated by large ^1H - ^1H homonuclear couplings, which obscure the much smaller chemical and Knight shifts. Despite this, valiant attempts to utilize the temperature and magnetic-field dependence of the broad ^1H line shape to extract average Knight-shift information have been made,^{14,15} but of course no locally resolved information was available. Hentsch *et al.*⁸ have employed multiple-

pulse homonuclear decoupling^{16,17} in combination with both magic-angle spinning (MAS) (Refs. 18 and 19) and single-crystal measurements to obtain local Knight-shift information on the protons in (fluoranthenyl)₂AsF₆. In this case, however, the isotropic Knight shifts were very small, on the order of -10 ppm, because of the small paramagnetic susceptibility of (FA)₂AsF₆. Furthermore, as the spin susceptibility of (FA)₂AsF₆ vanishes below the phase transition, no information concerning the metal-insulator transition could be gained.

In this paper we report variable-temperature high-resolution and broadline ¹H nuclear-magnetic-resonance measurements on DMTM(TCNQ)₂, which give insight as to the electronic and structural changes at the phase transition. In Sec. II we present high-resolution multiple-pulse MAS NMR measurements of Knight shifts of the proton resonances. Three inequivalent TCNQ ¹H lines are observed above *T_c* and eight below, all with large negative Knight shifts. The spin densities on the inequivalent sites are calculated, and a tentative assignment of the lines is made.

In Sec. III we present broadline ¹H NMR data showing that the DMTM disorder above *T_c*, inferred from the presence of the mirror plane in the x-ray structure, is dynamic in nature and that it arises from a combination of *trans*-form-*trans*-form conversion, methyl-group rotation, and at least one uncharacterized motion. We further show evidence for a cooperative phenomenon involving slow motions at *T_c*.

II. KNIGHT SHIFTS

A. Background

The nuclear resonance frequency is generally shifted relative to the Larmor frequency of a bare nucleus as a result of the local fields induced by the surrounding electrons. In the case of diamagnetic materials, the shift is due to the electronic shielding of the nucleus from the static magnetic field *B*₀ and is termed a chemical shift as it is closely correlated with the local chemical environment. In systems with conduction electrons, there is an additional shift, termed the Knight shift,⁷ which is a shift in the nuclear magnetic resonance due to the averaged hyperfine interaction of the conduction electrons with the nucleus.²⁰ As with the chemical shift, it is defined in a field-independent manner as *K* = Δ*ω*/*ω*₀, relative to the Larmor frequency *ω*₀. In general, it is a tensor quantity and is given by

$$\vec{K} = (\chi_s / \gamma_e \gamma_n \hbar) \vec{A}, \quad (1)$$

in which χ_s is the spin susceptibility either per conduction electron or per molecule, depending upon convention, γ_e and γ_n are the gyromagnetic ratios of the electron and nucleus, respectively, and \vec{A} is the hyperfine coupling tensor. The total shift tensor δ is the sum of the chemical- and Knight-shift tensors, which, in general, have different orientations with respect to one another. The separation of chemical- and Knight-shift tensor information from the spectrum, when their relative orientations are unknown, is problematic and in practice always

involves some assumptions. For a powder under magic-angle spinning conditions, in the fast spinning limit, the situation is dramatically simplified as only isotropic shifts remain. The total shift of the resonance position is then given by²¹

$$\delta_{\text{iso}} = \sigma_{\text{iso}} + K_{\text{iso}}, \quad (2a)$$

in which

$$K_{\text{iso}} = (\chi_s / \gamma_e \gamma_n \hbar) a_{\text{iso}}. \quad (2b)$$

Despite this simplification, the problem of how to separate the chemical and Knight shifts remain, and there are several methods in the literature which have been used. One possibility is to use a structurally similar neutral compound as a chemical-shift reference.^{12,13} This is the simplest approach as one only needs a single spectrum to obtain a value for *K*_{iso}, but its accuracy relies on the fact that the chemical shift of the structurally similar neutral species is identical to that of the charge-transfer complex. The use of a chemical-shift reference is less problematic for ¹H NMR than for ¹³C NMR, as the total range of ¹H chemical shifts is only ~10 ppm. The second approach is to use the dependence of the Knight shift on the paramagnetic susceptibility, either by reducing χ_s by progressive microwave saturation of the electronic spin system^{13,22,23} or by varying χ_s by performing temperature-dependent measurements.^{4,9} In the latter approach, plotting the shift versus χ_s (measured independently versus *T*) will give a line with a slope given by

$$\frac{\Delta \sigma_{\text{iso}}}{\Delta \chi_s} = (1 / \gamma_e \gamma_n \hbar) a_{\text{iso}}. \quad (3)$$

This approach can, in principle, be quite accurate when a wide temperature range is used so that the susceptibility is varied by a factor of 2–3 or more. When χ can only be varied over a range of 10–30 %, small errors in the susceptibility measurement, particularly when small numbers of data points are used, can lead to comparatively large errors in the slopes. In such a case, using a chemical-shift reference may be the more accurate approach. In this paper we have opted for a compromise. The spectra were acquired over as wide a temperature range as possible (190–300 K). Coupling constants were calculated using TCNQ as a chemical-shift reference and using Eq. (2b) with the published spin susceptibility as a function of temperature,²⁴ and the results at different temperatures were averaged. For the case of ¹H Knight shifts, which arise from the polarization of the 1s core electrons by the spin density on the directly bound carbon, the spin density on the bound carbon, ρ , may be simply calculated from the isotropic hyperfine coupling constant via the McConnell relation²⁵

$$a_{\text{iso}} / 2\pi = \rho Q, \quad (4)$$

in which *Q* is the McConnell constant, usually taken to be -66.4 MHz, for *sp*²-hybridized carbons.²⁶

B. ¹H Knight shifts in DMTM(TCNQ)₂

Figure 1 shows the ¹H spectrum of a powdered sample of DMTM(TCNQ)₂ under conditions of MREV-8

multiple-pulse decoupling^{27,28} and magic-angle spinning, at different temperatures. The spectra of Fig. 1 represent the highest-resolution ¹H spectra of an organic conductor ever published. The linewidths are 2–2.5 ppm, scaled, a factor of 2 larger than usual for a diamagnetic crystalline organic solid, but the dispersion of the lines is nearly an order of magnitude larger than the usual dispersion due to ¹H chemical shifts. Figure 1(a) was acquired above T_c , at 291 K, where four center bands are visible. The DMTM cation's CH₂ and CH₃ groups give rise to the intense line at -1 ppm, while the three upfield lines are due to the TCNQ protons. The TCNQ protons are clear-

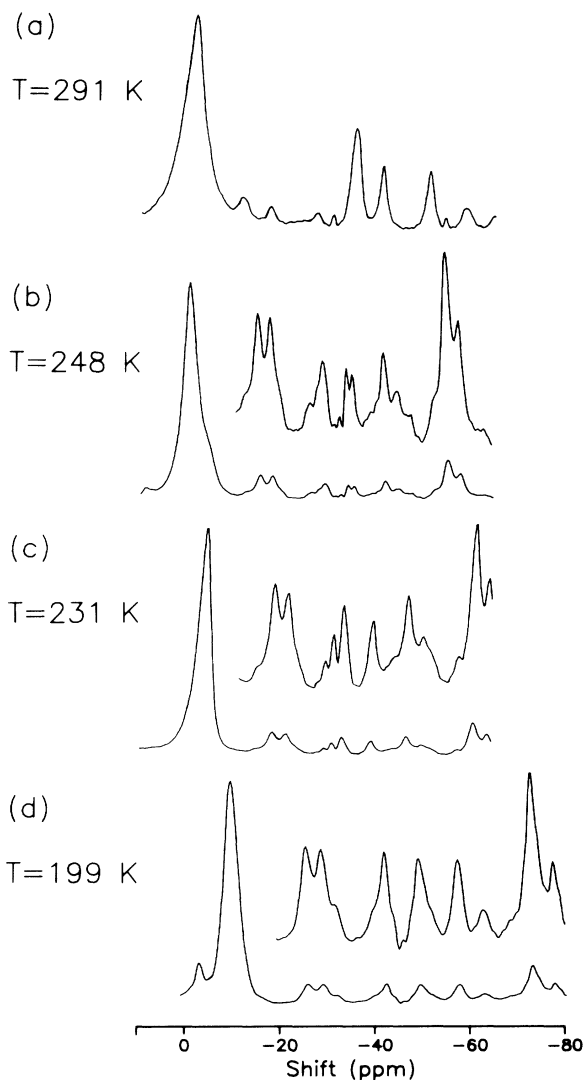


FIG. 1. ¹H MREV-8 MAS spectra of DMTM(TCNQ)₂. The ordinate axis is the MAS NMR intensity. The horizontal axis (abscissa) is ppm divided by the MREV-8 scaling factor $\kappa=0.471$ and is relative to tetramethyl silane (TMS). The ordinates in (b)–(d) represent vertical expansions by a factor of 5. The spectra are not corrected for phase transient effects. (a) $T=291$ K, the spinning speed was $\omega_r/2\pi=2.20$ kHz, and 16 scans were added; (b) $T=248$ K, $\omega_r/2\pi=4.10$ kHz, 88 scans; (c) $T=231$ K, $\omega_r/2\pi=4.40$ kHz, 128 scans, and (d) $T=199$ K, $\omega_r/2\pi=4.05$ kHz, 80 scans.

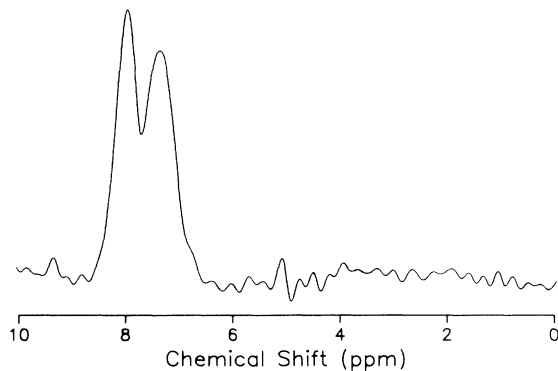


FIG. 2. High-resolution ¹H MAS spectrum of TCNQ acquired under homonuclear decoupling with BR-24. The ordinate axis is the MAS NMR intensity. The abscissa axis is ppm divided by the BR-24 scaling factor $\kappa=0.384$ and is relative to TMS. Two scans were added.

ly strongly Knight shifted—the spectrum of neutral TCNQ, are shown in Fig. 2, exhibits two partially resolved resonances at +8.06 and +7.44 ppm. The intensity ratio for the TCNQ protons, in Fig. 1(a), is 2:1:1; i.e., the line at -35 ppm represents two protons, equivalent to within our resolution. This spectrum was acquired at a relatively slow spinning speed $\omega_r/2\pi=2.2$ kHz, and one can see first-order rotational sidebands, of low intensity, in the range -10 to -30 ppm, due to the shift anisotropy of the TCNQ protons. The spectra below T_c were acquired at a higher spinning rate to avoid confusion among the rotational sidebands and the increased number of center bands. Below T_c there are nine center bands, eight of which correspond to TCNQ protons. One can see the resolution increase substantially with lowering temperature as the spread of isotropic Knight shifts increases. Figure 3 shows the shifts as a function of the temperature, for the eight TCNQ resonances below T_c and the three above. Note that all of the resonances have a temperature-dependent shift, which correlates well with the susceptibility, given as an upper nonlinear horizontal axis. The DMTM-cation resonance was used as a shift reference and was fixed at +1 ppm, to remove the effects of temperature-dependent phase transients, as discussed in Sec. IV, below. Though the spectra of Fig. 1 are uncorrected for this effect, all data discussed subsequently have been treated in this manner. The Knight shifts, hyperfine coupling constants, and corresponding local spin densities were calculated from Eqs. (2) and (4), using the center of the TCNQ resonance of Fig. 2, +7.75 ppm, as a chemical-shift reference, and the resulting data are tabulated in Table I. For these calculations χ_s was taken as the spin susceptibility per conduction electron, i.e., per TCNQ dimer. Some previous comparative studies of TCNQ salts have taken χ_s to be the susceptibility per TCNQ molecule, effectively normalizing the spin density to unity over one TCNQ, thus facilitating the comparison of results from TCNQ salts with differing degrees of charge per site.^{14,15,29} Care must be taken as to which convention has been used, in this regard, when comparing results from the literature.

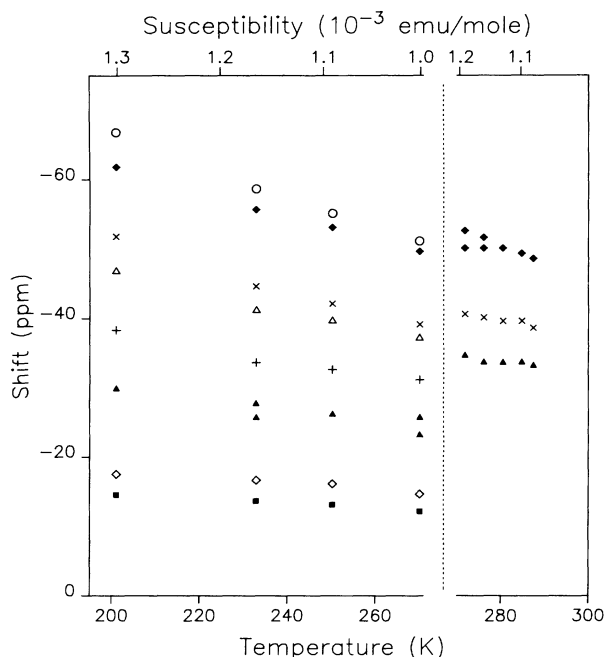


FIG. 3. ^1H line positions, for TCNQ protons, vs temperature. The upper horizontal axis is a nonlinear susceptibility scale. Shifts are given relative to TMS and are corrected for phase transients by fixing the DMTM cation resonance at +1 ppm. The dotted vertical line marks the phase transition at 272 K. Measurement errors are approximately ± 0.5 ppm. The lines are numbered in the text in the direction of increasing shift from TMS (from left to right in Fig. 1, excluding the intense leftmost signal assigned to the DMTM cation ^1H 's) as follows: above T_c , (1) solid triangle, (2) cross, and (3) solid diamond; below T_c , (1) solid square, (2) open diamond, (3) solid triangle, (4) plus, (5) open triangle, (6) cross, (7) solid diamond, and (8) open circle.

The first problem is explaining how one obtains three inequivalent lines above T_c , with the intensity ratio 2:1:1. INDO calculations, using the structure of the TCNQ molecule in $\text{DMTM}(\text{TCNQ})_2$ above T_c ,⁶ predict four ^1H lines, though the expected spread of the couplings, -1.34 to -1.38 MHz, is much smaller than observed in Fig. 1(a).³⁰ Clearly, the Knight-shift dispersion cannot be a feature of the geometric distortion of the TCNQ molecule alone, but must be related to the surrounding crystal field. This can perhaps be explained with the help of the crystal structure of Fig. 4(a). The labeled TCNQ of Fig. 4(b) is related, in the following discussion, to the center stack of Fig. 4(a) by a clockwise rotation. Note that the ^1H 's in positions 1 and 3 are oriented toward the TCNQ sheets, along the a axis, while the ^1H 's in positions 2 and 4 are pointing toward the DMTM cations in potentially different orientations. We propose that the protons in positions 1 and 3 are equivalent above T_c , within the resolution limit, for the comparatively small Knight-shift dispersion above T_c and give rise to the line at -35 ppm (corrected to -33 ppm) in Fig. 1(a), while the protons at positions 2 and 4 are differentially Knight shifted because of their different orientations with respect to the DMTM cation.

TABLE I. Hyperfine coupling constants and spin densities on the directly bound carbons for the TCNQ protons in $\text{DMTM}(\text{TCNQ})_2$. The first three lines are the resonances above the phase transition and the last eight are below. In both cases the lines are numbered in order of increasing shift from TMS, as in the caption to Fig. 3. Estimated errors are ± 0.1 MHz for $a_{\text{iso}}/2\pi$ and ± 0.001 for ρ . All data are averages and are based upon five points above T_c and four below. Symbols written $\langle a-b \rangle_{\text{av}}$, represent averages of the values for line Nos. $a-b$, preceding.

	Line No.	$a_{\text{iso}}/2\pi$ (MHz)	ρ
Above T_c	1	-1.8	0.026
	2	-2.0	0.030
	3	-2.4	0.037
	$\langle 1-3 \rangle_{\text{av}}$	-2.0	0.030
Below T_c	1	-0.9	0.014
	2	-1.0	0.015
	3	-1.5	0.022
	4	-1.8	0.027
	$\langle 1-4 \rangle_{\text{av}}$	-1.3	0.019
	5	-2.1	0.031
	6	-2.2	0.033
	7	-2.7	0.040
8	-2.8	0.042	
	$\langle 5-8 \rangle_{\text{av}}$	-2.4	0.036

The doubling of the number of TCNQ resonances from 4 to 8, while cooling through T_c , if we consider the line at -33 ppm in Fig. 1(a) to be two overlapping resonances, has also been observed in the ^{13}C MAS spectra of ^{13}C -1 labeled $\text{DMTM}(\text{TCNQ})_2$.⁴ The doubling of the number of CN resonances was attributed to the structural change at T_c , below which the two TCNQ stacks become ine-

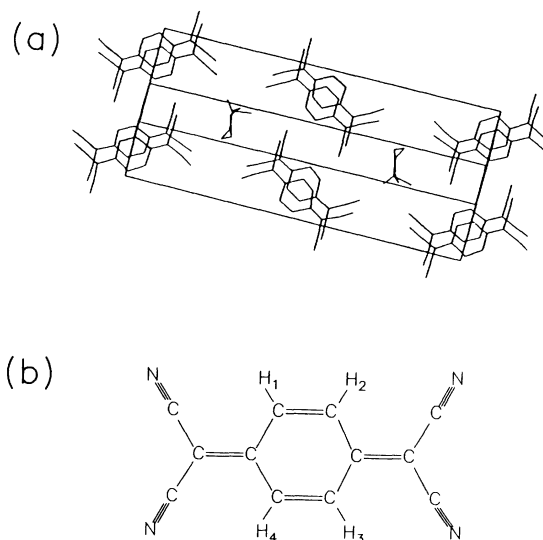


FIG. 4. (a) Schematic crystal structure of $\text{DMTM}(\text{TCNQ})_2$, above T_c , illustrating the dimerized TCNQ stacks. The DMTM counterions are disordered on a mirror plane between the two stacks (Ref. 1). (b) TCNQ with ^1H positions labeled.

quivalent.^{1,6} This assignment, supported by the x-ray structure work,^{1,6} seems to be a quite reasonable assignment of the ^1H lines below T_c reported here as well.

The average TCNQ hyperfine coupling constant $\langle a_{\text{iso}} \rangle_{\text{av}}$ may be obtained by averaging a_{iso} for lines 1 (weighted doubly), 2, and 3 above T_c , where $\langle a_{\text{iso}} \rangle_{\text{av}}/2\pi = -2.0 \pm 0.1$ MHz, and lines 1–8 below T_c , where $\langle a_{\text{iso}} \rangle_{\text{av}}/2\pi = -1.9 \pm 0.1$ MHz. These values are in good agreement with average values determined for other TCNQ salts using broadline methods.^{14,15} Though the average coupling constants and, correspondingly, the average spin densities are identical above and below T_c , the dispersion is substantially larger in the low-temperature phase. If we tentatively assign lines 1–4 in the low-temperature phase to one TCNQ stack and lines 5–8 to the other and calculate the average spin density for each stack, we obtain the results summarized in the $\langle \rangle_{\text{av}}$ rows of Table I. The average couplings and spin densities in rows labeled $\langle 1-3 \rangle_{\text{av}}$, $\langle 1-4 \rangle_{\text{av}}$, and $\langle 5-8 \rangle_{\text{av}}$ are the average of lines of Nos. 1–3 (above T_c with No. 1 weighted doubly), 1–4 (below T_c), and 5–8 respectively. Note that we can obtain the average spin densities $\langle 1-4 \rangle_{\text{av}}$ and $\langle 5-8 \rangle_{\text{av}}$ by subtracting and adding 0.009, respectively, to the average value above T_c , $\langle 1-3 \rangle_{\text{av}}$. This is consistent with the interstack electron transfer at T_c , proposed as an explanation for the conductivity anomaly.¹ The value of 0.009, interpreted as such, corresponds to an interstack transfer of 31% of the spin density, resulting in a relative charge distribution of 0.65–0.35 between the two stacks, in close agreement with the charge distribution (0.62–0.38) calculated from the isotropic ^{13}C -1 Knight shifts.⁴ Of course, these values depend upon the correct assignment of the lines, but this calculation places an upper limit on such a charge redistribution. The correlation of the ^1H lines, on the same stack, with each other could perhaps be made with the use of a two-dimensional spin-diffusion experiment.³¹

III. CATION MOTION IN DMTM(TCNQ)₂

The results reported in the previous section have all been obtained from high-resolution spectra, acquired via coherent averaging of the homonuclear dipolar interaction. This was necessary to reveal the underlying Knight shifts. A great deal of information can be obtained, however, from spectra dominated by large homonuclear couplings. The presence and rates of motion may be monitored by the change in the second moment of the proton spectrum with temperature, a feature which has been previously exploited to characterize the cation motion in other TCNQ salts.^{14,29} Since rapid spin diffusion equalizes the relaxation rates of the various ^1H 's, the measurement of relaxation rates versus temperature may yield information concerning the dominant relaxation mechanism, even if it involves a small number of protons. Two well-known examples are the ^1H spin-lattice relaxation of a macromolecule by a small number of rapidly rotating methyl groups³² and the relaxation of protons in an entire crystal by paramagnetic impurities on the order of a few percent.³³

Figure 5 illustrates the change in the second moment

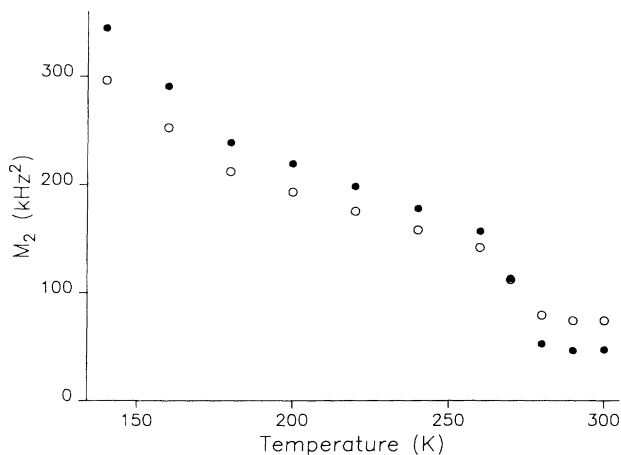


FIG. 5. Second moment of the ^1H static powder pattern vs temperature for DMTM(TCNQ)₂. Open circles are the raw data. Solid points are the adjusted data after subtracting contributions from the hyperfine interaction and the dipolar interaction among the TCNQ protons and scaling up to $\frac{1}{7}$.

of the ^1H powder spectrum as a function of temperature. The open circles represent the raw data, while the solid circles represent the data corrected for contributions to the second moment from other than the cation motion, as discussed below. The increase in the second moment, by a factor of 2, at the phase transition indicates a significant slowing of motion. As the TCNQ's are well defined in the x-ray structure, the motion does not involve them. The electron density of the DMTM cation, however, was only describable, after much effort, with a superposition of two models with occupancy 0.5.⁶ Analysis of the second moment of the ^1H spectrum can give an indication of the type of motion occurring in each temperature regime. Adapting the notion of Ref. 14, the second moment of the ^1H spectrum is given by

$$M_2 = \frac{4}{11}M_{2d}^Q + \frac{7}{11}M_{2d}^D + M_{2h} + M_{2d}^{DQ}, \quad (5)$$

in which M_{2d}^Q and M_{2d}^D are the contributions to the second moment from dipolar interactions among the TCNQ and DMTM protons, respectively, M_{2d}^{DQ} represents contribution from dipolar interactions between DMTM and TCNQ ^1H 's, and M_{2h} represents the contribution due to the hyperfine interaction of the protons with the conduction electrons. The prefactors weight the contributions by the relative number of protons involved. M_{2d}^Q should not vary much from one TCNQ salt to another and will be taken to be 56.2 kHz².¹⁵ M_{2d}^{DQ} is impossible to calculate exactly without knowing the details of the motion in advance, but it is estimated to be on the order of 5–8 kHz² or less and is therefore ignored. M_{2h} gives a temperature-dependent correction which can be calculated as in Refs. 14, 15, and 29, using the values $a_{\text{iso}}/2\pi = -2.0$ MHz, $d_Q/2\pi = 0.90$ MHz, calculated from the results of Sec. II. d represents the anisotropic electron-proton dipolar contribution to the hyperfine coupling tensor. d_Q is given by $d_Q \sim -a_Q/2.5$, and an estimate is made of $d_D/2\pi = 0.45$ MHz.^{15,34} Note that

these values are different by a factor of 2 from those of Refs. 14, 15, and 29 because of the differing spin-density normalization convention used, as discussed in Sec. II. B. These contributions in Eq. (5), were subtracted from the original data, which were then scaled up by $\frac{1}{7}$ to give the adjusted data, represented in Fig. 5 by the solid circles, which should have contributions only from M_{2d}^D . At low temperatures, below 200 K, the second moment is indicative of methyl-group rotation only. In the range 220–260 K, $M_2 = 150\text{--}200 \text{ kHz}^2$ and fits reasonably well to a model calculation involving methyl-group rotation and *trans-form*–*trans-form* conversion, which gives $M_2 \sim 145 \text{ kHz}^2$.¹⁴ The calculations were performed for MEM (methyl-ethyl morpholinium) (TCNQ)₂,¹⁴ but the differences in M_2 , from motional narrowing, due to the differences between MEM and DMTM, which amounts to the loss of one CH₂ group and the substitution of O with S, are expected to be minimal. The motion considered for the MEM calculation was π flips of MEM about an axis perpendicular to the N–O axis.¹⁴ As a *trans-form*–*trans-form* conversion in DMTM is topologically equivalent to a π flip about an orthogonal axis, the calculation should serve for this motion as well. Above T_c , M_2 drops to 45–50 kHz², indicating that another motion sets in. From the value of M_2 alone, one would be inclined to invoke full rotations of the cation, which is predicted to give $M_2 \sim 45\text{--}80 \text{ kHz}^2$.¹⁴ However, the x-ray results, in this case, would give a completely smeared out electron-density distribution for the DMTM's, which is not observed. Other motions which preserve the mirror plane include *trans-form*–*gauche-form* and *gauche-form*–*gauche-form* conversions and librations; however, in the absence of further data, we are unable to characterize this motion. This problem could, in principle, be addressed via ^2H NMR in combination with site-specific labeling.

Figure 6 illustrates the spin-lattice relaxation rate in the laboratory (solid triangles) and the rotating (solid circles)

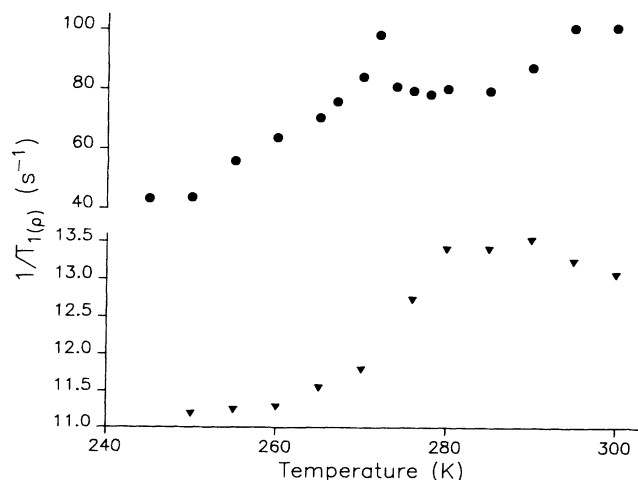


FIG. 6. Spin-lattice relaxation rates in the rotating (solid circles) and laboratory (solid triangles) frames vs temperature for DMTM(TCNQ)₂. Note the different vertical scales for $1/T_1$ and $1/T_{1\rho}$.

frames. Note the peak in $1/T_{1\rho}$ at T_c while cooling through the phase transition, after which the relaxation rate in the rotating frame drops precipitously. The peak in $1/T_{1\rho}$ corresponds to a peak in the low-frequency spectral density and is due to dramatically enhanced low-frequency fluctuations at T_c —a signature of a cooperative phenomenon involving slow motions. The principal relaxation mode, involving motions on the order of $2\omega_1/2\pi = 10^5 \text{ s}^{-1}$, also seems to vanish below T_c . An Arrhenius plot of the rotating-frame relaxation data below T_c yields an activation energy of $E_a = 13.6 \text{ kJ/mol}$, which is typical of a fairly free motion. This is likely to be *trans-form*–*trans-form* conversions as discussed above. The relaxation rate in the laboratory frame, $1/T_1$, has a step, but as this is dominated by fluctuating hyperfine fields produced by the conduction electrons, this has more to do with the electronic reorganization at T_c than molecular motion.

IV. EXPERIMENTAL DETAILS

DMTM(TCNQ)₂ was prepared by the reaction of the cation iodide with TCNQ in boiling acetonitrile, using the same technique as previously described for the other TCNQ complex salts.^{35,36}

The proton multiple-pulse MAS experiments were performed on a Bruker MSL-200 NMR spectrometer operating at a proton frequency of 200.1 MHz and equipped with a Bruker variable-temperature multiple-pulse MAS probe, with a quality factor of ~ 60 . The ^1H $\pi/2$ pulse length was 1.5 μs , and the MREV-8 cycle time used was 36 μs . The pulse length and phases were optimized using the method of Vaughan *et al.*³⁷ at Rhim *et al.*,³⁸ recently described by Gerstein.³⁹ The MREV-8 sequence was chosen for these experiments over BR-24,⁴⁰ because of the latter's limited spectral window and sensitivity to local fields, such as large shift dispersions.⁴¹ A word should be said about the effects of phase transients,³⁸ among other errors, which give rise to an additional precession about the effective field, i.e., a spurious resonance offset, in multiple-pulse experiments. The standard tune-up procedures include a minimization of such effects,^{37–39} though the frequency axis should be calibrated by acquiring a multiple-pulse spectrum of a reference sample with known ^1H chemical shifts. There are particular problems with experiments involving either variable-temperature and/or conducting samples, both of which can change this calibration. Experimentally, these effects may be minimized by using a probe with a low-quality factor (≤ 100) and watching for a degradation in the resolution with changing conditions. A second possibility is to include a diamagnetic compound in the sample as a resonance-offset reference, though this may not be feasible with a crowded spectrum. In this paper we have used the DMTM line as such a reference, as the DMTM line in the ^{13}C spectrum shows no temperature dependence.³ The actual DMTM line position changed from -2 to -12 ppm from 300 to 200 K and did not correlate well with the susceptibility. In all cases we have taken this to be $+1 \text{ ppm}$, typical for a diamagnetic CH₃ group. The effects of the phase transients on the multiple-pulse

scaling factor were considered to be minimal, as the resolution did not degrade over the temperature range investigated, and were therefore ignored.

The static ^1H measurements were performed on a homebuilt spectrometer operating at a proton frequency of 181.5 MHz. The probe was also homebuilt and typically used ^1H $\pi/2$ pulse lengths of $\sim 3 \mu\text{s}$. Spin-lattice relaxation measurements in the rotating and laboratory frames were performed with a variable-spin lock with $\omega_1/2\pi = 50$ kHz and an inversion recovery sequence, respectively, followed by detection with an echo. Echo decays as a function of time were monitored with a boxcar averager interfaced with the ASYST acquisition system (Asyst Software Technologies, Rochester, NY). Typically, 32 values of the decay time were measured with 4–20 scans per point. Time constants were extracted via direct fits to the exponential decays. Temperature control to ± 0.5 K was accomplished via an Oxford Instruments temperature controller (Oxford, England).

V. CONCLUSIONS

We have performed temperature-dependent high-resolution and broadline ^1H NMR measurements on the organic conductor DMTM(TCNQ)₂. The high-resolution spectra exhibit three strongly Knight-shifted lines, with intensity ratio 2:1:1, due to TCNQ protons above T_c and eight below. These spectra were explained in terms of the crystal structure and changes occurring at the phase

transition. The hyperfine couplings and corresponding spin densities were calculated, and a tentative assignment of resonances corresponding to two inequivalent stacks, with a relative charge distribution of 0.65–0.35, has been made. The broadline measurements confirm the model of cation motion as an important component of the phase transition. The second moment of the ^1H line, given by motionally averaged homonuclear couplings, displays a step at T_c , indicating the loss of a motional degree of freedom. The relaxation rate in the rotating frame exhibits a peak at the same temperature, indicating a cooperative transition involving slow motions. The Knight-shift and cation-motion results taken together seem to support a model in which, at T_c a DMTM-cation motion freezes out and the directed dipole moment of the DMTM cation aids in an interstack electron transfer. This makes the stacks electronically different and leads to a doubling of the number of the Knight-shifted lines in the ^1H spectra.

ACKNOWLEDGMENTS

We gratefully acknowledge the assistance of Dr. H. Förster at Bruker Analytische Messtechnik with the variable-temperature CRAMPS experiments. We thank Dr. M. Helmle for useful discussions and A. Werner for performing the INDO calculations. This research was supported by the Deutsche Forschungsgemeinschaft under Grant No. SFB 329. A.C.K. is supported in part by NSF and NATO.

- ¹R. J. J. Visser, S. Van Smaalen, J. L. De Boer, and A. Vos, *Mol. Cryst. Liq. Cryst.* **120**, 167 (1985).
- ²M. Almeida, L. Alcacer, S. Oostra, and J. L. De Boer, *Synth. Met.* **19**, 445 (1987).
- ³F. Rachdi, M. Ribet, P. Bernier, and M. Almeida, *Synth. Met.* **35**, 47 (1990).
- ⁴F. Rachdi, T. Nunes, M. Ribet, P. Bernier, M. Helmle, M. Mehring, and M. Almeida, *Phys. Rev. B* **45**, 8134 (1992).
- ⁵G. Zimmer, A. C. Kolbert, F. Rachdi, P. Bernier, M. Almeida, and M. Mehring, *Chem. Phys. Lett.* **182**, 673 (1991).
- ⁶R. J. Visser, J. L. De Boer, and A. Vos, *Acta. Crystallogr. C* **46**, 864 (1990).
- ⁷W. Knight, in *Solid State Physics*, edited by T. Seitz, and D. Turnbull (Academic, New York, 1956), Vol. 2, p. 93.
- ⁸F. Hentsch, M. Helmle, D. Königeter, and M. Mehring, *Phys. Rev. B* **37**, 7205 (1988).
- ⁹D. Königeter and M. Mehring, *Phys. Rev. B* **39**, 6361 (1989).
- ¹⁰M. Mehring and J. Spengler, *Phys. Rev. Lett.* **53**, 2441 (1984).
- ¹¹P. Bernier, M. Audenaert, R. J. Schweizer, P. C. Stein, D. Jerome, K. Bechgaard, and A. Moradpour, *J. Phys. Lett.* **46**, L675 (1985).
- ¹²M. Mehring, M. Helmle, D. Königeter, G. G. Maresch, and S. Demuth, *Synth. Met.* **14**, 349 (1987).
- ¹³M. Mehring, in *Low-Dimensional Conductors and Superconductors*, edited by D. Jerome and L. G. Caron (Plenum, New York, 1987), p. 185.
- ¹⁴S. Oostra, B. v.Bodegom, S. Huizinga, G. A. Sawatzky, G. Grüner, and J. P. Travers, *Phys. Rev. B* **24**, 5004 (1981).
- ¹⁵F. Devreux, Cl. Jeandey, M. Nechtschein, J. M. Fabre, and L.

Giral, *J. Phys. (Paris)* **40**, 671 (1979).

¹⁶M. Lee and W. I. Goldberg, *Phys. Rev.* **140**, A1261 (1965).

¹⁷J. S. Waugh, M. L. Huber, and U. Haeberlen, *Phys. Rev. Lett.* **20**, 180 (1968).

¹⁸E. R. Andrew, A. Bradbury, and R. G. Eades, *Nature* **182**, 1659 (1958).

¹⁹I. J. Lowe, *Phys. Rev. Lett.* **2**, 285 (1959).

²⁰Knight shifts in metals are considered to arise from averaged hyperfine couplings to conduction electrons moving at the Fermi velocity, in a metallic band. In this case the charges as well as the spins have a high mobility. In organic conductors, however, large paramagnetic shifts have been observed in systems with conductivities as low as $\sigma = 10^{-6}$ S/cm [A.C. Kolbert and M. Mehring (unpublished results)]. All that is necessary for such shifts is that the correlation time of the electron spins be shorter than the inverse of the hyperfine coupling. The charges, in such cases, are localized, while strong electron-electron couplings allow rapid spin diffusion, resulting in a high electron-spin mobility. The formalism describing such shifts is parallel to that of the Knight shift in metals. As the distinction between the two situations, in practice, is not always clear, we will continue to refer to such solid-state shifts, arising from averaged hyperfine couplings to electrons, as Knight shifts.

²¹There is often confusion at this point as to the sign conventions for the chemical and Knight shifts. This is due to the fact that chemical shifts to positive frequencies were originally defined as negative or *downfield* shifts, while Knight shifts to positive frequencies have been defined as positive. In the

- study of synthetic metals, which exhibit large chemical and Knight shifts, this leads to the absurd result that the sign of an observed spectral shift cannot be unambiguously reported unless the underlying physics has been unraveled. In this paper we have avoided the problem by defining positive-frequency shifts as positive, regardless of their origin. This convention is reflected in the form of Eq. (2a).
- ²²W. Stöcklein, H. Seidel, D. Singel, R. D. Kendrick, and C. S. Yannoni, *Chem. Phys. Lett.* **141**, 277 (1987).
- ²³R. A. Wind, H. Lock, and M. Mehring, *Chem. Phys. Lett.* **141**, 283 (1987).
- ²⁴S. Oostra, J. L. De Boer, and P. De Lange, *J. Phys. (Paris) Colloq.* **44**, C3-1387 (1983).
- ²⁵H. M. McConnell and D. B. Chestnut, *J. Chem. Phys.* **28**, 107 (1958).
- ²⁶P. H. Rieger and G. Fraenkel, *J. Chem. Phys.* **37**, 2795 (1962).
- ²⁷P. Mansfield, *J. Phys. C* **4**, 1444 (1971).
- ²⁸W.-K. Rhim, D. D. Elleman, and R. W. Vaughan, *J. Chem. Phys.* **59**, 3740 (1973).
- ²⁹J. P. Travers, F. Devreux, and M. Nechtschein, *J. Phys. (Paris) Colloq.* **44**, C3-1295 (1983).
- ³⁰A. Werner (private communication).
- ³¹P. Caravatti, P. Neuenschwander, and R. R. Ernst, *Macromolecules* **18**, 119 (1985).
- ³²V. D. Fedotov and H. Schneider, in *NMR Basis Principles and Progress*, edited by Diehl, Fluck Gunter, Kosfeld and Seelig, (Springer, Berlin, 1990), Vol. 21, p. 107.
- ³³A. Abragam, *Principles of Nuclear Magnetism* (Oxford University Press, New York, 1961).
- ³⁴J. Avalos, F. Devreux, M. Guglielmi, and M. Nechtschein, *Mol. Phys.* **36**, 669 (1978).
- ³⁵M. Almeida and L. Alcacer, *J. Cryst. Growth* **62**, 183 (1983).
- ³⁶M. Almeida, L. Alcacer, and A. Lindegaard-Andersen, *J. Cryst. Growth* **72**, 567 (1985).
- ³⁷R. W. Vaughan, D. D. Elleman, L. M. Stacey, W.-K. Rhim, and J. W. Lee, *Rev. Sci. Instrum.* **43**, 1356 (1972).
- ³⁸W.-K. Rhim, D. D. Elleman, L. B. Schreiber, and R. W. Vaughan, *J. Chem. Phys.* **60**, 4595 (1974).
- ³⁹B. C. Gerstein, *Philos. Trans. R. Soc. London A* **299**, 521 (1981).
- ⁴⁰D. P. Burum and W.-K. Rhim, *J. Chem. Phys.* **71**, 944 (1979).
- ⁴¹A. Bielecki, A. C. Kolbert, H. J. M. deGroot, R. G. Griffin, and M. H. Levitt, *Adv. Magn. Reson.* **14**, 111 (1990).